

Simulation-Based Evaluation of Sliding Mode Control with Washout Filter for Power Balancing in Battery Energy Storage Systems

¹Sikander Hans, ²Balwinder Kumar, ³Surya Kant Singh, ⁴Amit Bishnoi

¹Principal, Department of Electrical Engineering, KC group of Research & professional institute, Pandoga, Una

²Principal, Department of Electrical Engineering, KC Polytechnic, Pandoga, Una

³Vice-Principal, Department of Electrical Engineering, KC group of Research & professional institute, Pandoga, Una

⁴Assistant Professor, Department of Electrical Engineering, KC group of Research & professional institute, Pandoga, Una

dr.sikanderhans@gmail.com

Abstract: This research paper presents a simulation-based evaluation of a novel sliding mode control (SMC) approach with a washout filter for power balancing in battery energy storage systems (BESS). Unlike traditional proportional-plus integral control methods, the proposed SMC technique is specifically tailored for charging and discharging BESS units. The primary objective of this study is to investigate the efficacy of the proposed SMC-based scheme in achieving optimal power balancing at the DC bus of the BESS. A comparative analysis is conducted to assess the performance of the developed SMC strategy against the conventional proportional-plus integral controller. MATLAB simulations utilizing Simulink and the Sim Power System toolbox are employed to obtain comprehensive results. The findings of this study provide valuable insights into the effectiveness of the SMC with washout filter for enhancing power balancing in BESS applications, thereby contributing to advancements in energy storage system control methodologies.

Keywords: Sliding Mode Control (SMC), Washout Filter, Power Balancing, Battery Energy Storage Systems (BESS), Simulation-based Evaluation, MATLAB Simulation

1. INTRODUCTION

Fast depletion of limited to fuel resources more carbon emission and huge transmission losses are focusing the concern of power sector companies towards the use of renewable energy resources (RES). Renewable energy resources are the sources which can be achieved from the boundless source[1]. Appropriate use of renewable energy resources is popular discussion going nowadays. It is exceptionally fundamental to pick which source of energy we should be utilized and why we need to use it? Greater part of components for example, neatness, cost, stability, proficiency and natural impacts must be considered. It is a harsh reality that, numerous productions far and wide are as yet needy on non-renewable energy sources for power generation. Presumably, these energizes are extremely successful to the extent control generation quality is concerned; however over the long haul they are not beneficial. Non-renewable energy sources will drain one day and the enterprises must turn to inexhaustible sources as quickly as time permits [2-3]. Additionally, these petroleum derivatives represent a colossal danger to ecological parity and are a reason for some natural risks.

Among all the renewable resources, solar power source is the successful contenders because of kind highlights, for example, accessibility of sun on earth, simplicity of establishment, improve of maintenance, moving parts unavailable, and insignificant dirtiness level etc. One of the important disadvantages of solar system is unpredictable nature of sun light due to rotation of earth and bad climate condition[4]. This issue can without much of a stretch be understood by using a mixture comprising of a photovoltaic cluster and a battery. This course of action gives consistent, continuous and autonomous power supply to the framework load. The hugest element of renewable power source is its ample supply. Renewable power sources are clean source of energy that have an a lot lesser negative ecological effect than customary fossil vitality advancement [5].

Uses of renewable power sources are comprehensively performed on-grid and off-grid. A framework is essentially a coordination of production, transmission and circulation which supplies power to purchasers[6]. On-grid and off-grid are the terms which portray the manner in which power is conveyed. On-grid manages power stations which are straightforwardly associated with grids, for example, wind turbine and sun oriented boards. Off-grid applications, by and large, serve just one burden, for example, a little home or a town house, charging batteries for electric vehicle, organizations can depend on on-grid solar systems to meet their every day necessities, as well as gain pay from the overabundance power created and on splendid radiant days, structures can produce enough sunlight based power to control machines, lights, water warming frameworks, etc. Off-grid applications can take numerous structures, from solar PV modules for a singular town home to unified windmills to control a town, water siphon or a

business battery charging office or charging station for electric vehicles. These off-grid applications are most commonly utilized in remote or on the other hand rustic settings [7]. A noteworthy on-lattice application is to create power in mass sums.

The world is moving towards electric vehicles as a substitute wellspring of fuel vehicles, in this manner diminishing the impact of a worldwide temperature alteration and concern over greenhouse gases[8]. Likewise, fuel vehicles are consuming over 50% of the fuel assets, resulting in the bringing about the generation of a lot of ozone depleting substances. The day isn't far when these conventional resources will depleted completed if the utilization of these resources keeps on being expended at a similar rate[9]. In this way, there is an incredible requirement for redevelopment of the transportation part to have less reliance of human being on conventional sources. Hence, electric vehicles should be operated by clean, energy productive sources, for example, a battery with the goal that the reliance on non-renewable power sources limits. Thusly, numerous nations over the world are effectively taking part and checking out the redesign of the vehicle area and moving towards electric vehicles [10].

Reason behind moving from fuel vehicles toward electric vehicles (EVs) is the quick increment in the crude oil price and carbon emission[11]. However, if there should be an occurrence of plug-in hybrid vehicle the battery is charged through the grid or renewable power sources, for example, photovoltaic, wind, fuel cell. Energy storage device, for example, batteries are frequently related in renewable energy producing framework because renewable power sources are helpless to weather factors which result in unpredictable production of power and unbalanced supply of power [12]. With the developing worry about a worldwide temperature alteration, nations have started to target lessening ozone harming substance outflows. With the end goal of ecological security and fuel cost decrease, automobile producers have put incredible endeavors into creating electric vehicles (EVs). Soon, EVs are relied upon to be the standard of the transportation division .

To combine energy storage device with the renewable energy sources, a DC-DC bidirectional converter is normally utilized in a renewable energy producing system. A DC-DC bidirectional converter operates in two modes.

- Charging Mode
- Discharging Mode

When the renewable power resources generate more than the power demanded by load then surplus power will stored in the battery and this is called charging mode. Oppositely when the renewable power resources generate lower than the power demanded by load then power flows from battery to the load and required power by the load comes through storage device and this is called discharging mode. For the charging

process, if the DC link capacitor voltage is less from the voltage of battery, in this case system will step up the voltage and battery will charge, else if DC link capacitor voltage is greater from the voltage of the battery then system will step down the voltage and battery will charge. For the discharging process, if the voltage of DC link capacitor is less from the voltage of battery, in this case system will step down the voltage and battery will discharge, else if the voltage of DC link capacitor is greater from voltage of battery than system will step up the voltage and battery will discharge [13].

2. LITERATURE REVIEW

The literature review on problems with control of DC-DC bidirectional buck-boost converter is briefly summarized.

- It has explained and designed a fuzzy logic controller based DC-DC buck-boost converter and performed this controller on MATLAB/Simulink. In this controller designed a FLC and a feedback added. An irregular output voltage is contrast with the reference voltage and produced error signal. This error signal is run by the fuzzy logic controller then fuzzy logic controller is contrast with the saw tooth carrier wave to generate pulse width modulation signal which runs the MOSFETs[14]. Also, the results of FLC are compared with the conventional proportional-plus integral controller and have proposed that FLC has better response than proportional-plus integral controller.
- Used a proportional-plus integral control technique to charge and discharge the battery for electrical vehicle. In this system a grid to vehicle and vehicle to grid power transferred by utilizing DC-DC bidirectional buck-boost converter or single phase ac/dc bidirectional converter. Converter has conveyed the alternating current from the grid and AC current to the grid at UPF and reduced harmonics which eventually delays the life of converter and the storage device[15].
- It has proposed a deliberate methodology of the deduction of nonisolated TPC topography designed for combining an inexhaustible source, a storage device and a load at the same time. The energy flow in triple port converter has investigated and then applied on dual input converters and dual output converters. In this system explained a triple port converter attributes and which results in high efficiency and high assimilation[16].
- It has designed another nonisolated buck-boost type 5-level DC-DC converter reasonable for higher power and higher voltage application. In this system displayed the fundamental highlights of this topology are: lower voltage over the semiconductors and diminished volume of output channel. The

hypothetical investigation is completed for a multilevel bidirectional structure of that converter. The designed topology displays a few capacitors and their voltage level should be fit for legitimate activity of the converter. In this manner, a capacitor voltage adjusting dynamic control utilizing a feed forward procedure is proposed and broke down in detail. So as to approve the hypothetical investigation, a model with 10 kW output control capacity[17].

- Explained a power leveling framework is connected to keep up a harmony between power supply and such an unpredictable control age. The PLS is required to work charge or release of capacity and bidirectional power stream. Accordingly the PLS comprises of a bidirectional buck-boost DC-DC converter. In this investigation, the bidirectional buck-boost DC-DC converter and twofold electric layer capacitor are connected to the PLS. The yield current of power leveling system is controlled so as to keep control parity and DC transport voltage. PLS ought to work control leveling rapidly for prompt change of intensity age framework[18]. In this examination, Control of the DC-DC Converter applying to miscreant (DB) control dependent on linearization is proposed to acquire fast reaction.
- The primary objective of this paper is to structure and investigate a bidirectional drifting interspaced DC-DC buck-boost converter connected to a private photovoltaic control framework with vitality stockpiling. The drifting interspaced bidirectional converter produces a higher DC voltage addition contrasted with customary converters, decreasing the required number of arrangement associations for the solar photovoltaic and battery system. This paper demonstrates a transitional control technique from grid connected to islanded working modes, just as the back association with the buck-boost working modes for the bidirectional DC-DC converter. The paper portrays the DC connect the board and voltage control where the guideline strategies are shown by investigation and re-enactment results appearing total framework activity[19].
- Few electrical topography of circulated stockpiling units are portrayed by the utilization of bidirectional converters that store in a battery bank at specific minutes and supply this to micro grid transport when essential. The OCC (open-cycle control) system has been utilized in the exchanging converters to enable quick reaction to homeless people, no overshoots and zero relentless state mistake. The target of this work is to utilize OCC procedure in a bidirectional Buck-Boost converter to charge a battery bank when they are released, and to supply the battery power to the load when important, guaranteeing insurance to the load and to the storage device[20].

- In numerous grid associated applications a DC-DC exchanging converter is generally associated between the solar photovoltaic arrays and the dc-ac converter. This paper shows an improvised technique to structure a sliding mode controller for the solar photovoltaic framework, which runs the photovoltaic voltage to pursue a reference given by an outer maximum power point tracking calculation and mitigates the annoyances brought about by the irradiance changes and motions in the mass voltage. By taking into account that the exchanging surface is the straight mix of the input capacitor current and the photovoltaic voltage blunder, the designed plan displays preferences in examination with existing arrangements that depend in the linearization of internal current circle elements[21]. The designed basic topology, by considering the impacts in the shut circle framework elements of a reference channel, guarantees a stable sliding routine in all the ideal task scope of the framework, while the settling time, what's more, overshoot of the solar photovoltaic voltage required by a maximum power tracking calculation are given.

3. DESIGN OF COMPONENTS OF THE PROPOSED SYSTEM

3.1 Design of Solar Photovoltaic Array

Representation of a sunlight based PV cell, consisting of a current source with diode in parallel[22]. At the output side series resistor (R_s) and shunt resistor (R_p) are associated. The identical circuit of a sunlight based photovoltaic cell is displayed below.

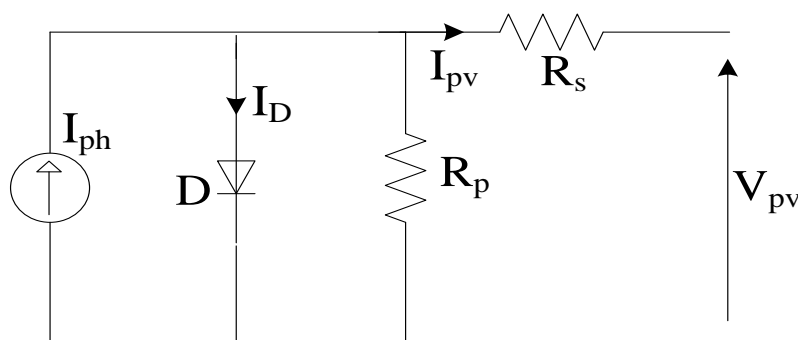


Fig. 2.3 Equivalent circuit of photovoltaic cell

The design of solar PV panel is modelled by the equation given below:

$$I_{pv} = n_p I_{ph} - n_p I_{sat} \left[\exp \left(\left(\frac{q}{AKT} \right) \left(\frac{V_{pv}}{n_s} + I_{pv} R_s \right) \right) - 1 \right] \quad (2.1)$$

$$I_{ph} = \left(I_{SSO} + k_i(T - T_r) * \frac{s}{1000} \right) \quad (2.2)$$

$$I_{sat} = I_{rr} \left(\frac{T}{T_r} \right)^3 \exp \left(\left(\frac{qE_{gap}}{kA} \right) * \left(\frac{1}{T_r} - \frac{1}{T} \right) \right) \quad (2.3)$$

where I_{pv} is Photovoltaic current, n_p & n_s is Number of cells in parallel and series, I_{ph} is photocurrent, I_{sat} is reverse saturation current, q is electron charge which is 1.602×10^{-19} C, A is ideality factor, K is Boltzman constant which is 1.38×10^{-23} J/K, T is temperature of the PV, V_{pv} is photovoltaic voltage, R_s is series resistance of PV cell, I_{SSO} is short-circuit current, k_i is short circuit current temperature coefficient, T_r is Reference temperature which is 300 K, s is Solar irradiation level, I_{rr} is Reverse saturation current at T_r , E_{gap} is Energy of the band gap for silicon which is 1.12 eV [23].

The peak power capacity of solar PV array is considered around 1.4kW in this work[24]. As indicated by structure consideration one solar module has V_{oc} of 53.9V and I_{sc} of 3.41A. The general equation of an active (P) power for solar photovoltaic is given below,

$$P_{maxM} = V_{mppM} * I_{mppM} \quad (2.4)$$

$P_{max} = (85\% \text{ of } V_{oc} * 85\% \text{ of } I_{sc})$ thus I_{mppM} is 2.89A and V_{mppM} is 45.89V of every module. The measured peak power is give below,

$$P_{maxM} = V_{mppM} * I_{mppM} = 1442W \quad (2.5)$$

It demands peak input voltage of 122.4V and peak input current of 11.78A equivalent to maximum power of 1442W, to reach up to this voltage ($122.4/53.9$) and current ($11.78/2.89$) 3 modules are associated in series and 4 are associated in parallel respectively [25]. V_{oc} is open circuit voltage, I_{sc} is short circuit current, P_{max} is maximum power, V_{mpp} is maximum voltage, I_{mpp} is maximum current.

3.2 Design of DC-DC Boost Converter

The DC-DC boost converter is constructed to increase the voltage and the maximum voltage is followed by IC (Incremental conductance) control method [26] which is 122.4V and this voltage is boosted up to 380V. Parameters of the boost converter are as per following:

$$L_b = \frac{V_{pv}D}{2\Delta i_1 f_{sh}} \quad (2.6)$$

$$D = 1 - \frac{V_{in}}{V_b} \tag{2.7}$$

Where L_b is input inductor, D is duty cycle, $V_{in} = V_{pv}$ is solar PV output voltage, Δi_1 is input current ripple and f_{sh} is the switching frequency.

$$V_{in} = V_{pv} = 122.4V \text{ to } V_{dc} = 380V \tag{2.8}$$

The measured value of D is 0.678 and for this converter value of f_{sh} is 10KHz and input current ripple is considered as 10% of input current I_1 .

$$I_1 = P/V_{in} = 11.78A \text{ and } \Delta i_1 = 1.178A \tag{2.9}$$

The value of input inductor L_b is calculated and selected slightly higher value as 5mH

3.3 Modelling of Battery Energy Storage

Batteries are an important element in any standalone PV system. As different sorts of batteries are accessible in the market[27]. Most regularly connected in EVs among all are the lithium-ion batteries because of huge energy thickness, long- life stable operation. Equivalent circuit of lithium-ion batteries is displayed in Fig. 2.4.

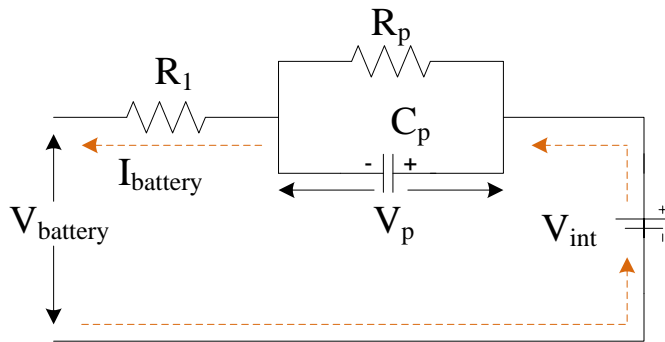


Fig. 2.4 Model of Lithium Ion Battery

- Where: R_p = parasitic resistance
- C_p = parasitic capacitance
- V_{int} = internal voltage
- R_1 = internal resistance

When the battery is energized the parallel RC network appeared in Fig. 2.4 depicts the transient state of the battery [28]. Subsequently, there will be a few reductions happening over the internal resistance of the battery during this situation. Along these lines, voltage over the battery isn't equal as that of internal battery voltage. Fig. 2.5 shows equivalent circuit of the battery.

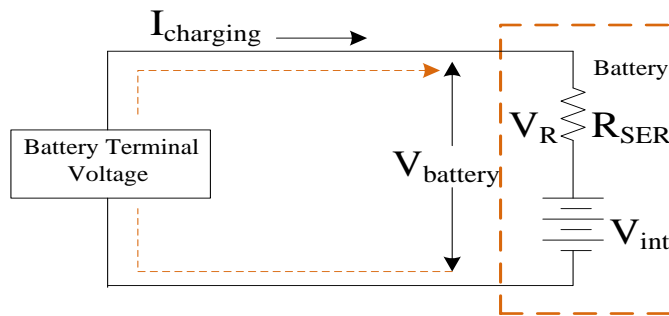


Fig. 2.5 Equivalent Circuit of Battery

$$V_R = I_{charging} * R_{SER} \tag{2.10}$$

Therefore,

$$V_{battery} = V_R + V_{int} \tag{2.11}$$

Hence,

$$V_{battery} = V_{int} + I_{charging} * R_{SER} \tag{2.12}$$

Also, cell charge battery voltage is given as,

$$V_{battery} = \frac{1}{C_{cell}} \int I_{charging} dt + V_{int} + I_{charging} * R_{SER} \tag{2.13}$$

The maximum cut-off voltage of the lithium-ion battery $V_{Battery\ cutoff}$ can be calculated using equation (2.13) as,

$$\Delta t = \frac{1}{I} (V_{battery\ cutoff} - V_{int} - V * C) \tag{2.14}$$

Hence, equation (2.14) represents the charge time taken by the battery. Here, V_{int} is the initial battery voltage before charging, R_{SER} is the series equivalent resistance of the battery

4. DESIGN OF SLIDING MODE CONTROLLER BASED ON WASHOUT FILTER

As to obtain the ideal task of battery, a DC-DC buck-boost bidirectional converter is utilized[29]. A SMC based on washout filter is utilized to control I_b . Battery storage converter is planned to keep up power stability of the system and the battery is viewed as a perfect DC voltage source. Fig. 3.3 shows the simplified model of solar PV-battery model. By this we can calculate bus current (i_{bus}) and equivalent resistive load (R_{eq}).

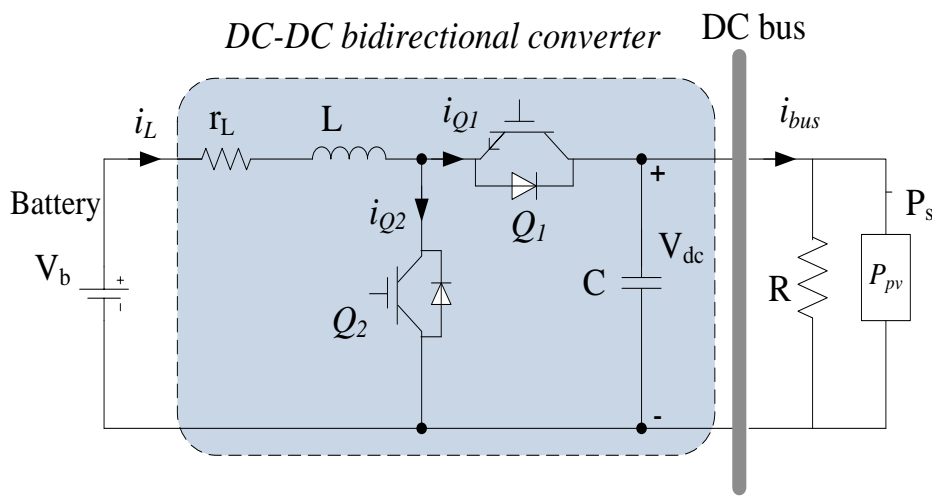


Fig. 3.3 Simplified model of PV-battery model

$$i_{bus} = \frac{V_{dc}}{R} + \frac{P}{V_{dc}} \tag{3.10}$$

$$R_{eq} = \frac{V_{dc}}{i_{bus}} \tag{3.11}$$

This equation can create two situations, in first, when the generated power is greater than or equal to the power demand then load can directly feeds through source power; mean $\{|P_s| \geq |P_L|\}$. In second, when the generated power is less than power demand than a small disturbance can occur in voltage and current; means $\{|P_s| < |P_L|\}$. [30]

So the equivalent load is not linear and because of the varieties in accessible energy source, load can fluctuate over a wide scope of bends. That’s why a nonlinear examination is required for a stable operation.

The dynamics of this model can be represent as

$$\frac{di_L}{dt} = \frac{1}{L} [V_b - r_L i_L - u V_{dc}] \tag{3.12}$$

$$\frac{dV_{dc}}{dt} = \frac{1}{C} \left[u i_L - \frac{V_{dc}}{R} - \frac{P}{V_{dc}} \right] \tag{3.13}$$

In which, u is a control input modeled for switches Q1 and Q2. We assume when Q1 switch is on then Q2 is off and when Q2 is on then Q1 is off. Therefore $u \in \{0,1\}$.

The dynamics can be simplified by scaling the system in amplitude and time.

As $t = \tau \sqrt{LC}$ and $\{i_L, V_{dc}\} = \left\{ \sqrt{\frac{C}{L}} V_b x, V_b y \right\}$ respectively.

$$\frac{dx}{d\tau} = 1 - bx - uy \tag{3.14}$$

$$\frac{dy}{d\tau} = ux - ay - \frac{d}{y} \tag{3.15}$$

Where $a = \frac{1}{R} \sqrt{\frac{L}{C}}$; $b = \sqrt{\frac{C}{L}} r_L$; $d = \sqrt{\frac{L}{C}} \frac{P}{V_b^2}$

Where P is the variation between generated power and load demand as $P_{BES} = P = P_S - P_L$

The Sliding Mode Control based on Washout filter is provided all together to accomplish the following targets:

- (1) To regulate DC bus voltage
- (2) To reduce the transient response during the changing load
- (3) To guarantee robustness under changes.

When the standardized inductor current x is gone through a washout filter then we get another signal x_F .

Transfer function of x_F is given as,

$$G_F(s) = \frac{X_F(s)}{X(s)} = \frac{s}{s + \omega_n} = \frac{1 - \omega_n}{s + \omega_n} \tag{3.16}$$

Where ω_n is the cut off frequency of this filter. In this way, the consideration of the filter include to equation an extra differential condition given by,

$$\frac{dz}{dx} = \omega_n(x - z) \tag{3.17}$$

Where $z = x - x_F$. Representation of the sliding surface which utilized is given as follows.

$$h_n = y - y_r + k_n(x - z) \tag{3.18}$$

Where y_r is the desired DC link voltage, k_n is positive scalar control parameter, z is the lower frequency part of signal x . Control input u for switch control is given as,

$$u = \begin{cases} u^+ = 1, & \text{if } h_n(x) > \mu \\ u^- = 0, & \text{if } h_n(x) < -\mu \end{cases} \tag{3.19}$$

Where μ is constant which limits the hysteresis band is expressed as,

$$\mu = \frac{V_b(V_{dc} - V_b)}{2Lf_sV_{dc}} \tag{3.20}$$

Now it's important to denormalize the factors of the system.

$$\omega = \frac{\omega_n}{\sqrt{LC}} \tag{3.21}$$

$$k = k_n \sqrt{\frac{L}{C}}$$

After all the parameters have been resolved, the estimations of those parameters are at that point connected in the control block. Calculated parameters are as follows

- C = 50 μ F (Capacitance)
- L = 2.5mH (Inductance)
- r_L = 5m Ω (Inductor series resistance)
- f_s = 100kHz (Switching frequency)
- μ = 0.3796A (Hysteresis band)
- V_b = 196V (Battery voltage)
- V_{dc} = 380V (DC link capacitor voltage)

ω = 283rad/s (cut-off frequency)

k = 10 (scalar parameter)

Q = 150Ah (Battery capacity)

5. SIMULATION AND RESULTS

Results of the isolated solar PV-battery power producing system and grid connected system for electric vehicle are explained in this segment. Isolated system includes solar photovoltaic array, boost converter, BESS (bidirectional power flow) and resistive load. Grid connected system for electric vehicle includes solar photovoltaic array, boost converter, BESS (bidirectional power flow) and AC grid connected through bidirectional AC-DC converter.

5.1 ISOLATED SOLAR PV BATTERY SYSTEM:

MATLAB simulation is performed to prove the SMC based on washout filter in the isolated system. Results are obtained as the comparison of conventional proportional-plus integral control method with sliding mode controller based on washout filter.

5.1.1 Case study: There are three cases which have been performed. Table 4.1 shows the system parameters planned for the simulation.

5.1.1.1 Performance of the system with variation in solar irradiance: Depending upon the solar irradiance, power generated by the solar panel is vary with time. For these changes, various irradiance values for the solar-PV input power are simulated for this case. The main reason behind this case is to check the response of sliding mode controller whether it can give better response when the solar power is fluctuated. The peak power capacity of solar PV array is considered around 1.4kW in this work and the load is 210 Ω . The total time of simulation run is 035s. Fig. 4.1 shows the output plot of PV module at 500 W/m² & 1000 W/m². Power balance in this case is as, when the irradiance is high that time load feeds through PV power and the surplus power goes in battery and when PV irradiance is low then PV generates less power and has insufficient power to feed the load, at that time load feeds through battery.

Table 4.1 System parameters for simulation design

Sr. No.	Parameters	Value	Units
1.	Solar PV power (P_{pv})	1.4	kW
2.	Capacitance (C)	50	μF
3.	Inductance (L)	2.5	mH
4.	Inductor resistance (r_L)	5	$m\Omega$
5.	Hysteresis band (2δ)	0.3796	A
6.	Battery voltage (V_b)	196	V
7.	Initial capacitor voltage (V_c)	196	V
8.	Cut-off frequency (ω)	283	rad/s
9.	Scalar control parameter (k)	10	-
10.	Battery capacity (Q)	150	Ah

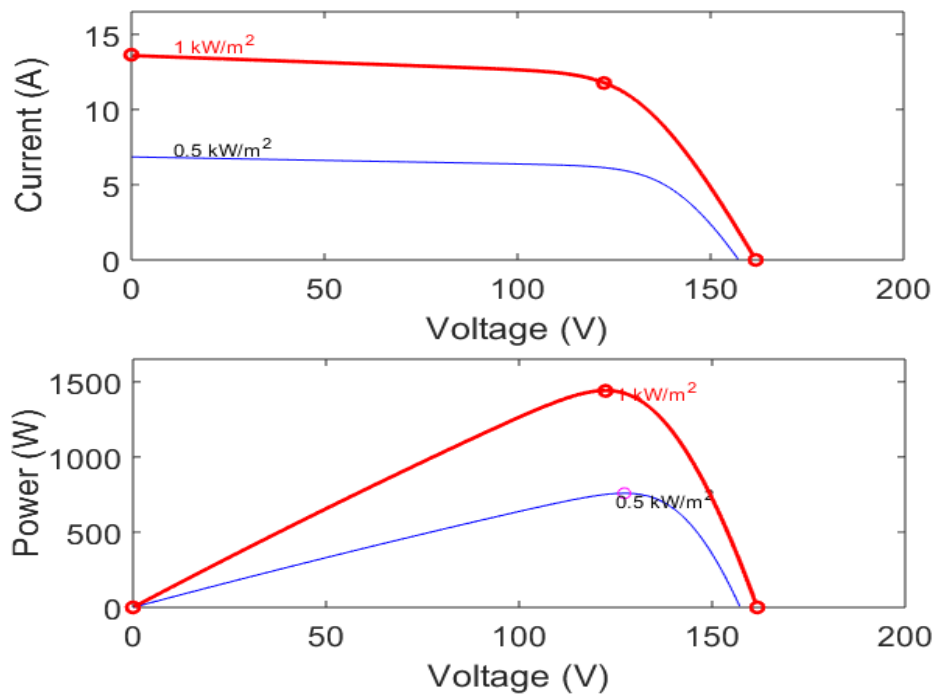


Fig. 4.1 P-V and I-V Characteristics of Solar photovoltaic Array

Results of the output voltage of DC link capacitor shown in fig. 4.2. Battery energy storage can mark the bus voltage with the variation in solar photovoltaic array. Inductor current simulation result is shown in figure 4.3. In this the Proportional-plus integral control moreover induces the comparative outcome with the Sliding mode control, main distinctive is proportional-plus integral control generates additional oscillation with the Sliding mode control when the transients occur. In Fig. 4.1 & 4.2 SMC drawn with red line and PI drawn with dashed blue line.

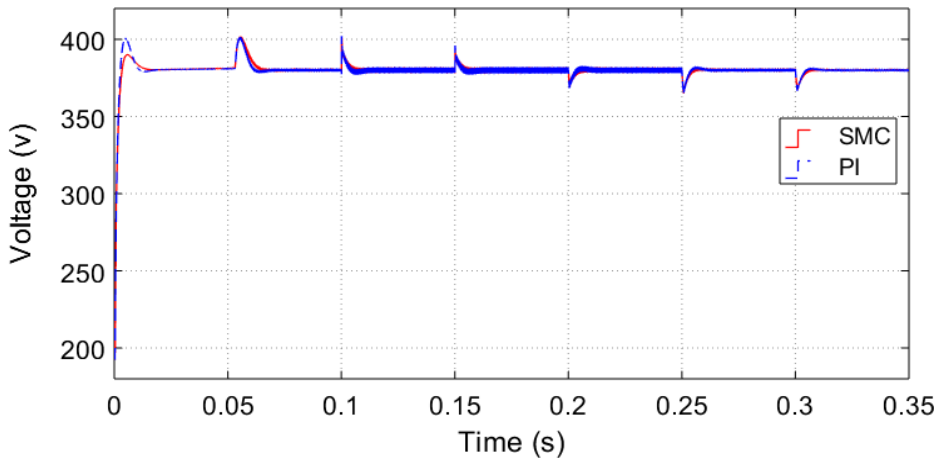


Fig. 4.2 Output voltage of DC link capacitor

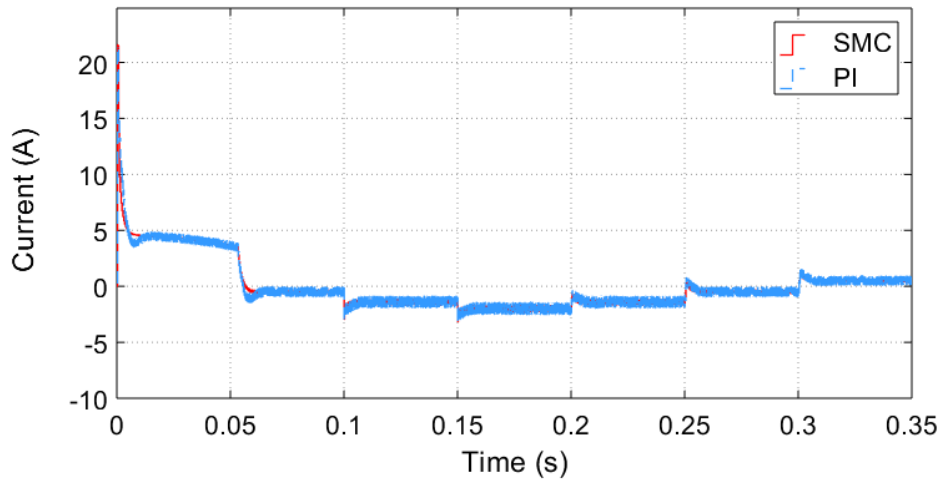


Fig. 4.3 Inductor current Results

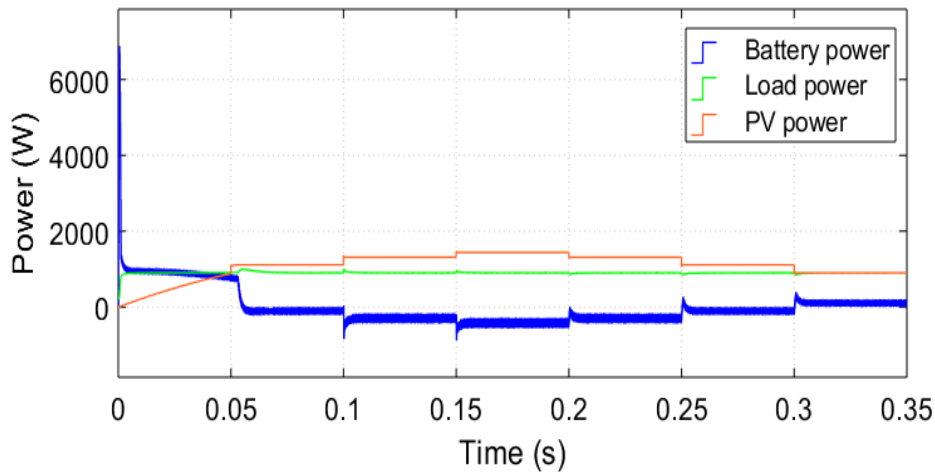


Fig. 4.4 Power Balance in Standalone Solar PV System

Fig. 4.4 shows the power balance in standalone mode. Consumption of the load power is around 657 W. Solar power, Battery power and load power drawn with red, blue and green respectively.

5.1.1.2 Regulation of Voltage at DC Link with SMC and PI: In this case the load is set as 160Ω and simulation time to run it up to 0.05sec. These result shows there is no overshoot in SMC when we compare it with PI and also SMC has faster settling time than PI. Fig. 4.5 shows DC link capacitor output voltage and Fig. 4.6 shows the inductor current results. PI drawn with dashed blue line and SMC drawn with red line.

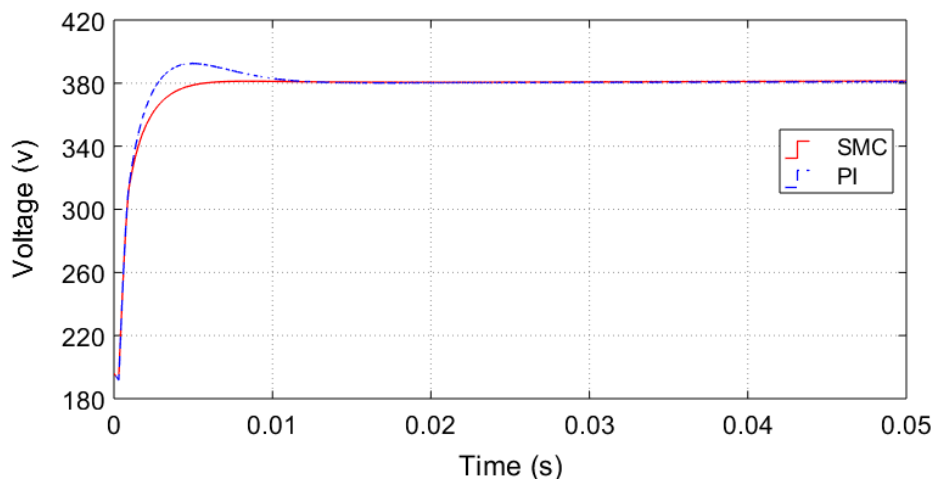


Fig. 4.5 Output voltage of DC link capacitor

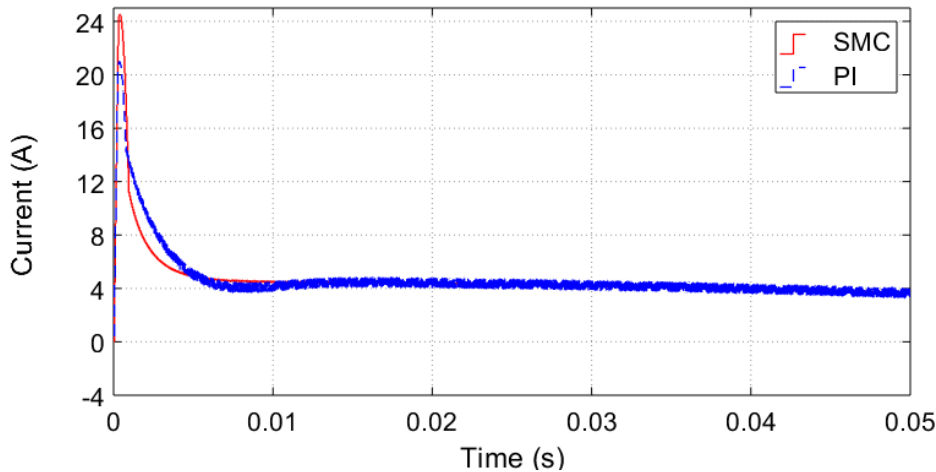


Fig. 4.6 Inductor current Results

5.1.1.3 Performance of the system with variation in load: The result of load variety is examined in this section. In this case the load resistance will change the value as 350Ω , 250Ω , 150Ω , 250Ω and 350Ω sequentially with the time duration of 01sec and the total simulation time is 0.5s. Fig. 4.7 shows the DC link capacitor voltage and Fig. 4.8 shows the inductor current result. We can see when the resistance load is minimized then voltage dip is occurring in result and when resistance load is maximized then voltage swell is occurring. When the overshoot voltage and undershoot voltage is occur SMC has a little better results than PI control.

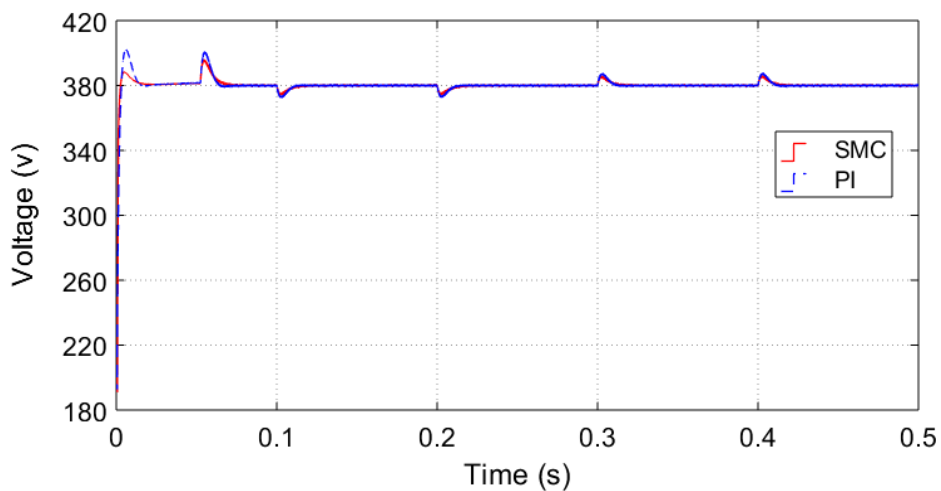


Fig. 4.7 Output voltage of DC link capacitor

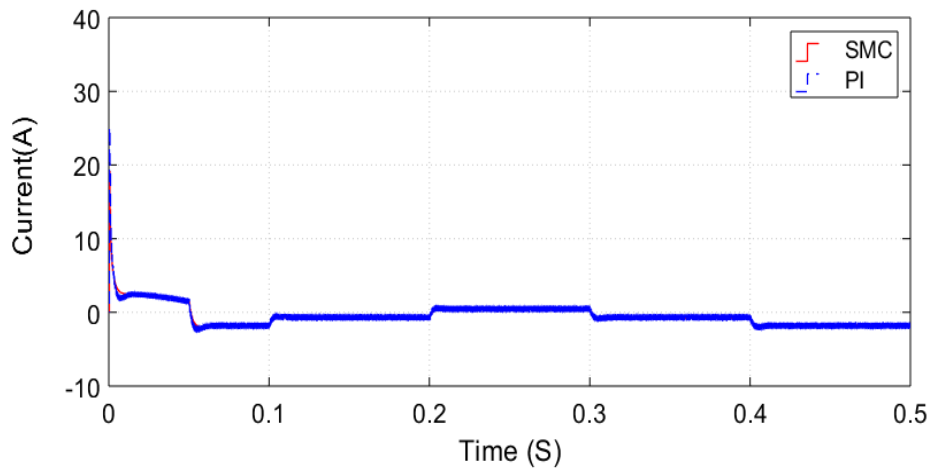


Fig. 4.8 Inductor current Results

5.2 GRID CONNECTED SYSTEM FOR ELECTRIC VEHICLE:

MATLAB simulation is performed with the SMC based on washout filter for the controlling of bidirectional DC-DC buck-boost converter. Results are obtained as variation in solar irradiance and battery %SOC.

5.2.1 Case study: There are two cases based on %SOC which have been performed. Table 4.2 shows the system parameters planned for the simulation

Table 4.2 System parameters for simulation design

Sr. No.	Parameters	Value	Units
1.	Solar PV power (P_{pv})	1.4	kW
2.	Capacitance (C)	50	μF
3.	Inductance (L)	2.5	mH
4.	Inductor resistance (r_L)	5	$m\Omega$
5.	Hysteresis band (2δ)	0.3796	A
6.	Battery voltage (V_b)	196	V
7.	Initial capacitor voltage (V_c)	196	V
8.	Cut-off frequency (ω)	283	rad/s
9.	Scalar control parameter (k)	10	-
10.	Battery capacity (Q)	150	Ah
11.	Grid voltage (V_{grms})	230	V
12.	Frequency (Hz)	50	Hz
13.	Inductor at AC side (L_{ac})	2.1	mH
14.	DC bus voltage (V_{dc})	380	V

5.2.1.1 Case 1: Battery is fully charged

In this case variation in solar PV irradiance level is 1000 W/m^2 and 500 W/m^2 and the battery %SOC is 100% means battery is already charged. In this case waveforms depicts as if the solar irradiance level is at 1000 W/m^2 and battery %SOC is 100% means, PV should feeds the AC grid and at 500 W/m^2 or PV has less power than power should be flow from battery to grid. In both of cases bidirectional AC-DC converter should works in inverting mode. In this case if the battery is already fully charged then we can see the discharging process of the battery into the grid. Fig. 4.9 shows the starting and steady state response of solar PV current, voltage and power. Fig. 4.10 shows the dynamic behavior of the system. Varying irradiance level of solar PV is shown in Fig. 4.10. Fig. 4.10 demonstrates the tracking of voltage at

maximum power point under different irradiance level. Fig. 4.10 depicts that if the irradiance of the solar PV is going to decrease then solar PV current (I_{pv}) and solar PV power (P_{pv}) is also decreased with constant solar PV voltage (V_{pv}). Fig. 4.10 also demonstrates that when solar irradiance level going to decrease battery current is increased because at this point power flow from battery to grid and battery is going to discharge.

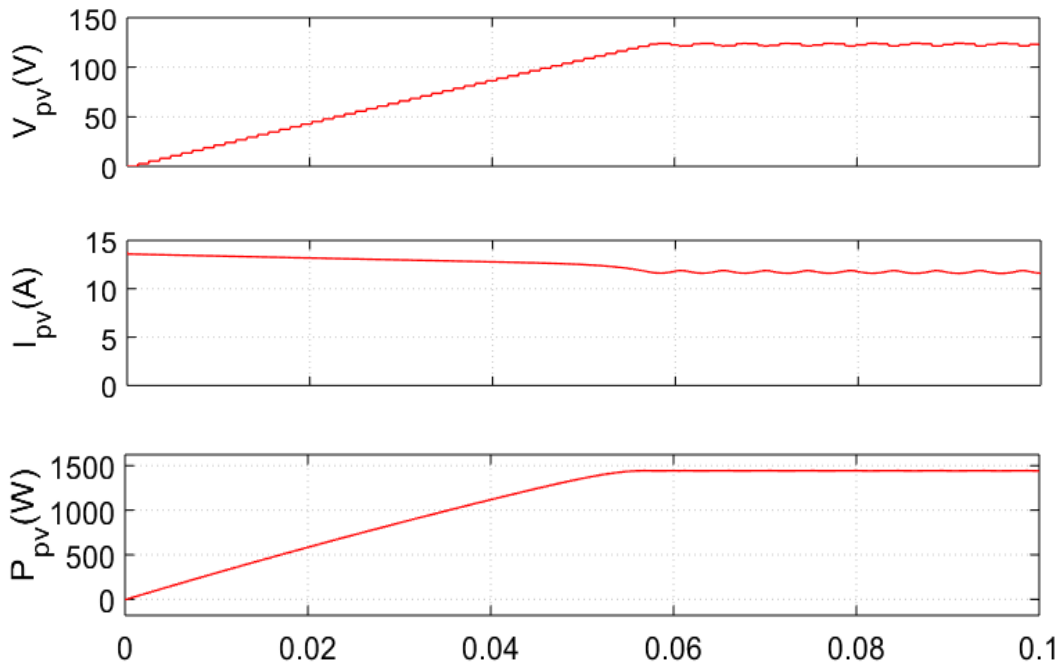
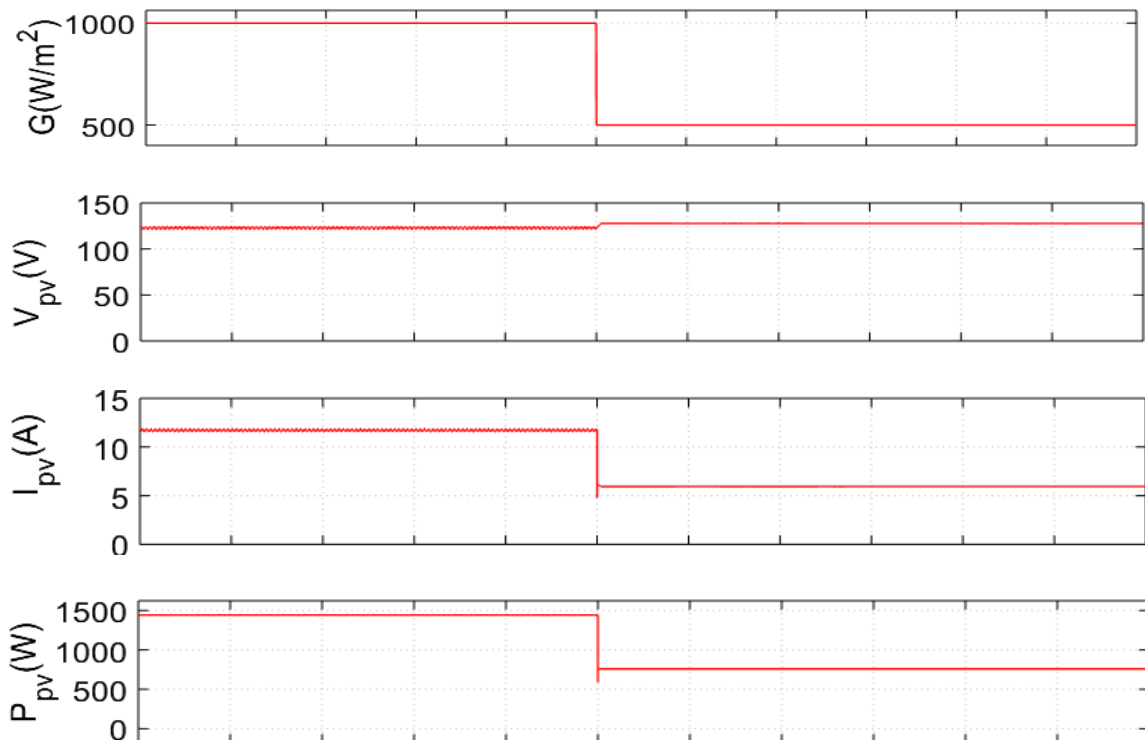
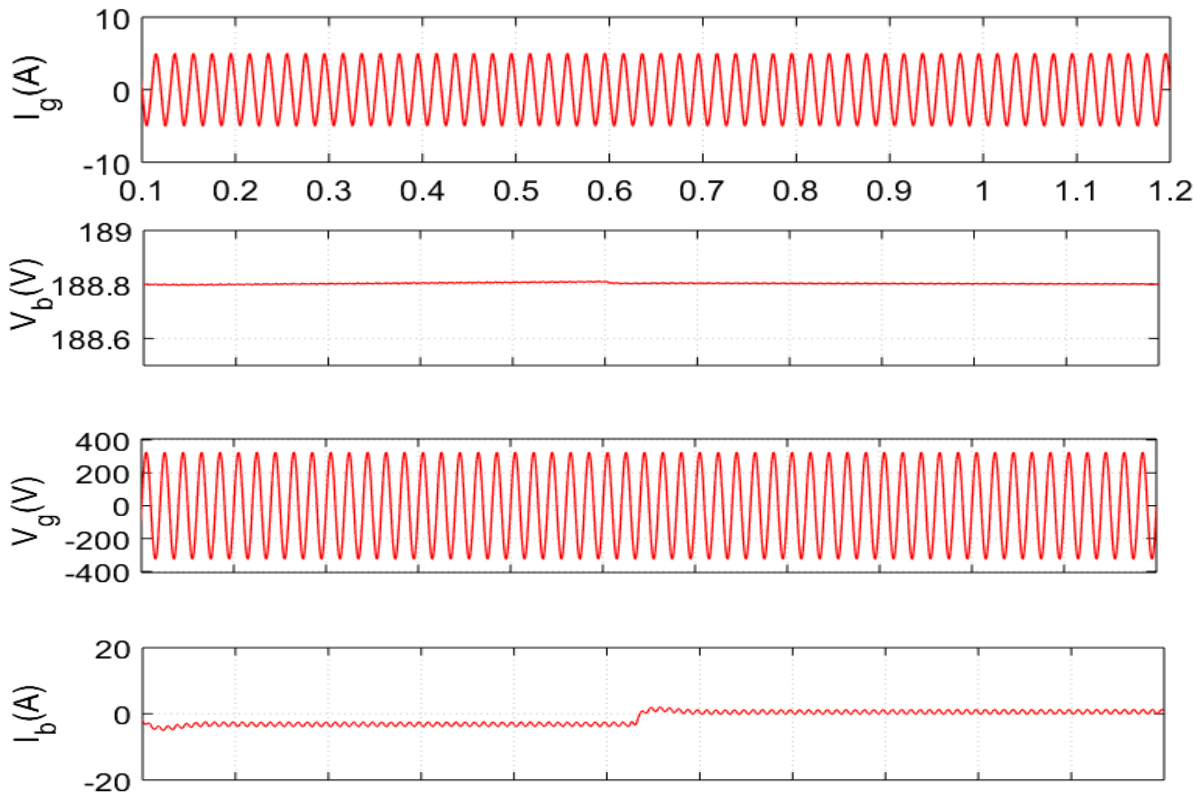


Fig. 4.9 starting response of PV current, voltage and power



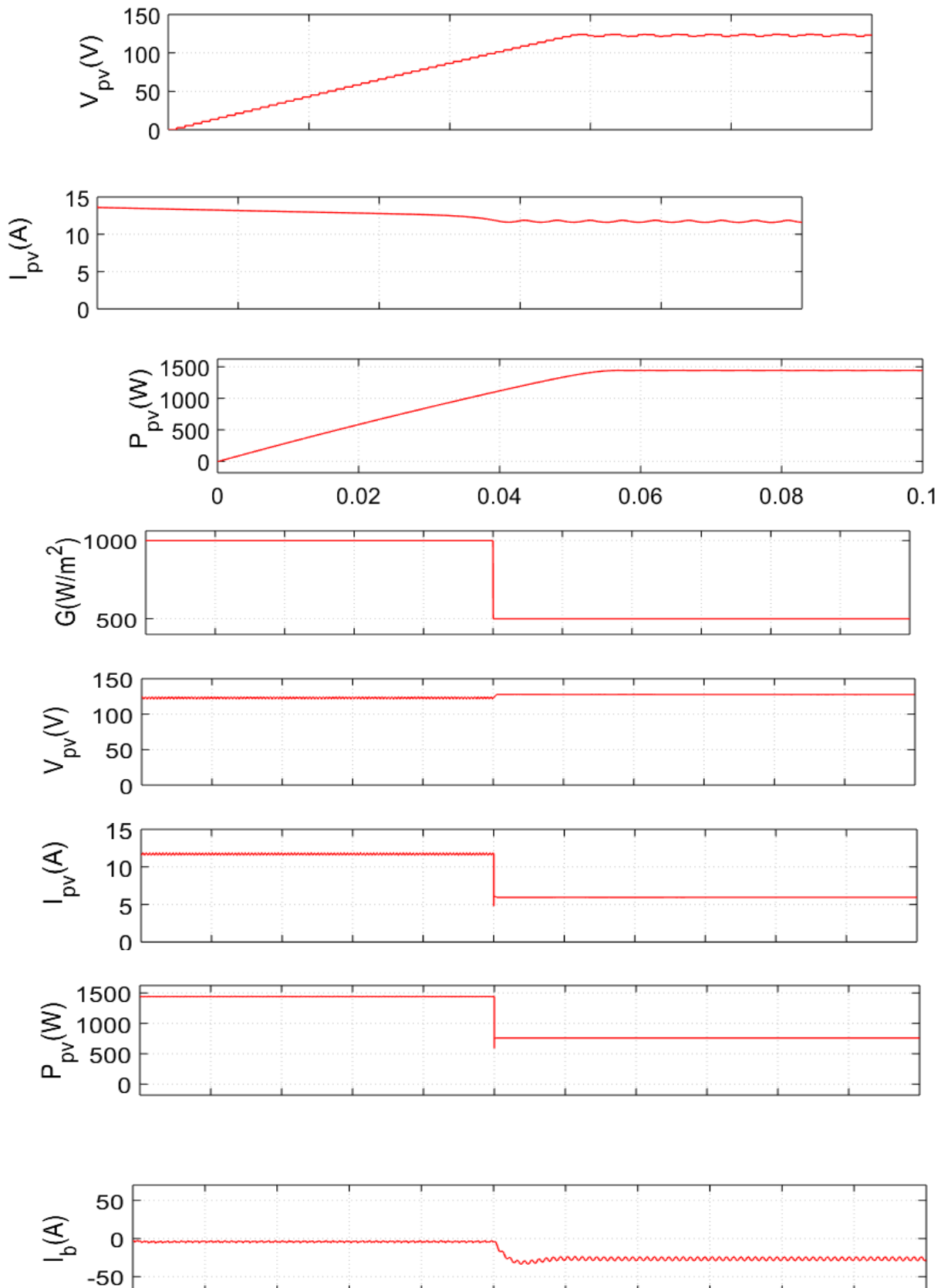


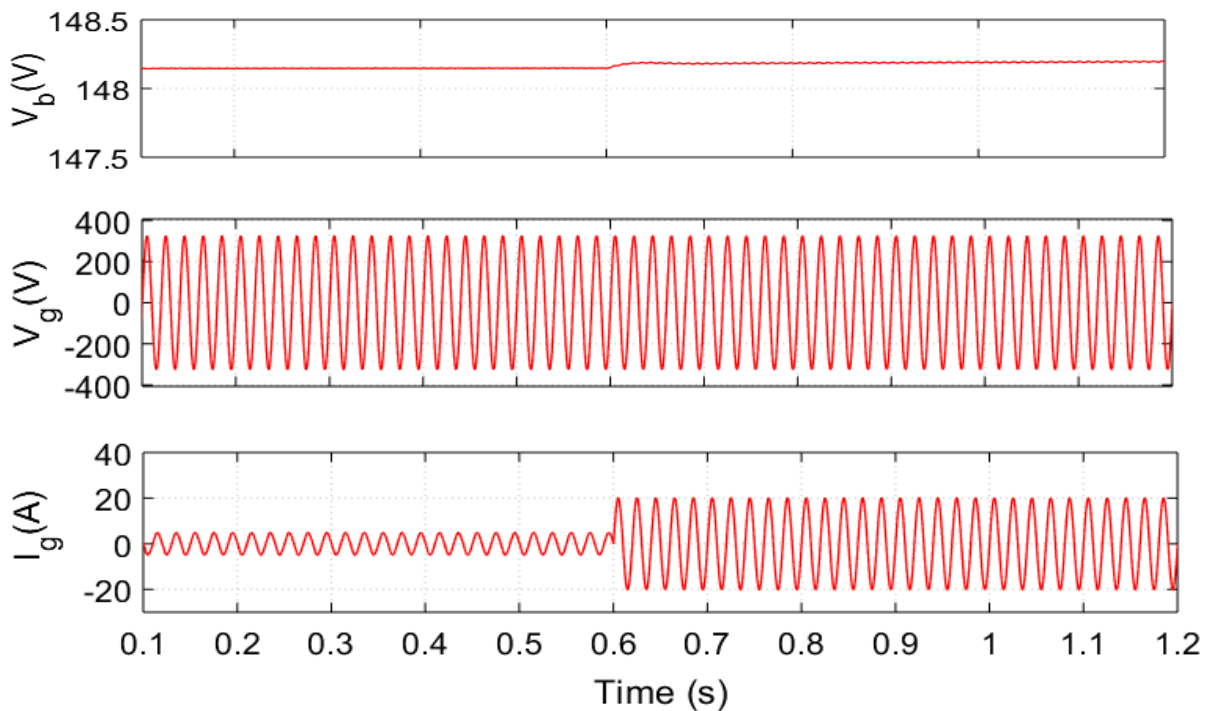
4.10 Dynamic response of system parameters under varying irradiance and SOC is 100%

4.2.1.2 Case 2: Battery is discharged

In this case variation in solar PV irradiance level is 1000 W/m^2 and 500 W/m^2 and the battery %SOC is 20% means battery is already discharged. In this case waveforms depicts as if the solar irradiance level is at 1000 W/m^2 and battery %SOC is 20% means, PV should feeds the battery and surplus power should go in AC grid, and at 500 W/m^2 or PV has less power than power should be flow from grid to battery. When PV irradiance level is 1000 W/m^2 than bidirectional AC-DC converter should works in inverting mode, and when PV irradiance level is 500 W/m^2 bidirectional AC-DC converter should works in rectifying mode, means power should flow from grid to battery. In this case if the battery is already discharged then we can see the charging process of the battery from the grid. Fig. 4.11 shows the starting and steady state response of solar PV current, voltage and power. Fig. 4.12 shows the dynamic behavior of the system. Varying irradiance level of solar PV is shown in Fig. 4.12. Fig. 4.12 demonstrates the tracking of voltage at maximum power point under different irradiance level. Fig. 4.12 depicts that if the irradiance of the solar PV is going to decrease then solar PV current (I_{pv}) and solar PV power (P_{pv}) is also decreased with constant solar PV voltage (V_{pv}). Fig. 4.12 also demonstrates that when solar irradiance level going to decrease

battery current is also decreased because at this point power flow from grid to battery and battery is going to charge.





4.12 Dynamic response of system parameters under varying irradiance and SOC is 20%

7.CONCLUSION

In this work, a novel strategy for battery charging and discharging is adopted to keep the stable operation of bidirectional DC-DC buck-boost converter in standalone solar PV-Battery system with DC loads, and in grid connected system for electric vehicle. A SMC based on Washout Filter is executed. For the execution of SMC, a MATLAB Simulation model has been directed. Through the control of bidirectional DC-DC buck boost converter for the battery charging and discharging process, Sliding Mode Control method with Washout Filter can keep the stable operation of the DC bus and maintain the power balance of the system. Firstly, SMC has been implemented on isolated solar PV-battery system then it is implemented with grid connected system for electric vehicles. SMC gives a superior reaction on the transients in cases of variable solar irradiation or the consumption of the loads is changing, compared to the conventional Proportional-plus Integral method. Sliding Mode Control provides better results in compared with PI Control on voltage overshoot and voltage undershoot.

REFERENCES

- [1] Elliott, R. T., Choi, H., Trudnowski, D. J., & Nguyen, T. (2022). Real power modulation strategies for transient stability control. *IEEE Access*, 10, 37215-37245.
- [2] Nandi, M., Shiva, C. K., & Mukherjee, V. (2019). A moth–flame optimization for UPFC–RFB-based load frequency stabilization of a realistic power system with various nonlinearities. *Iranian Journal of Science and Technology, Transactions of Electrical Engineering*, 43, 581-606.
- [3] Liu, Z., Yang, J., Jiang, W., Wei, C., Zhang, P., & Xu, J. (2019). Research on optimized energy scheduling of rural microgrid. *Applied Sciences*, 9(21), 4641.
- [4] SHAREEF, H. Artificial Intelligent Based Damping Controller Optimization for the Multi-Machine Power System: A Review.
- [5] Song, X. (2023). Machine Learning assisted Digital Twin for event identification in electrical power system (Vol. 34). *BoD–Books on Demand*.
- [6] Gusev, Y. P., & Subbotin, P. V. (2019, March). Using battery energy storage systems for load balancing and reactive power compensation in distribution grids. In *2019 International Conference on Industrial Engineering, Applications and Manufacturing (ICIEAM)* (pp. 1-5). IEEE.
- [7] Bragard, M., Soltau, N., Thomas, S., & De Doncker, R. W. (2010). The balance of renewable sources and user demands in grids: Power electronics for modular battery energy storage systems. *IEEE Transactions on Power Electronics*, 25(12), 3049-3056.
- [8] Huang, W., & Qahouq, J. A. A. (2014). Energy sharing control scheme for state-of-charge balancing of distributed battery energy storage system. *IEEE Transactions on Industrial Electronics*, 62(5), 2764-2776.
- [9] S.Katyal, S.Raina and S. Hans. "A Brief Comparative Study of Solar Energy." *International Journal for Scientific Research and Development* 5.4 (2017): 2126-2132.
- [10] S. Hans, S. Gupta Algorithm for Signature Verification Systems National conference on Signal & Image Processing(NCSIP-2012), Sri sai Aditya Institute Of Science & Technology.
- [11] S. Hans, S. Gupta Preprocessing Algorithm for Offline signature System" National Conference on Recent Trends in Engineering & science (NCRTES- 2012), Prestige Institute of Engineering & science, Indore.
- [12] S. Hans, An Algorithm for Speed Calculation of a Moving Object For visual Servoing Systems International Conference on VLSI, Communication and Networks (VCAN-2011), Institute of Engineering & Technology Alwar-2011.
- [13] S. Hans & SG Ganguli (2012) Optimal adaptive Visual Servoing of Robot Manipulators
- [14] S. Katyal, S. Raina and S. Hans. "A Energy Audit on Gujarat Solar Plant Charanka." *International Journal for Scientific Research and Development* 5.4 (2017): 2133- 2138
- [15] S. Hans (2018) A Review of Solar Energy And Energy Audit on Harsha Abacus Solar Plant: A Energy Audit on Gujarat Solar Plant Charanka.
- [16] S. Hans, R. Walia ,Thapar Institute of Engineering and Technology, Patiala. "Optimal MPPT Control using Boost Converter for Power Management in PV- Diesel Remote Area ." *Global Research and Development Journal For Engineering* 45 2019: 24 - 31.
- [17] Alka Rani , Deepam Sharma, Priyanka, Savita , Suryakant Singh and Sikander Hans. "ChatGPT's Possibilities in Advancing Education in the Age of Generative Artificial Intelligence: A Review and Analysis", *IJSREM*, 7(10) ,2023.

- [18] Hans, S. and Ghosh, S.(2020), "Position analysis of brushless direct current motor using robust fixed order H-infinity controller", *Assembly Automation*, Vol. 40 No. 2, pp. 211-218.
- [19] S. Hans and S. Ghosh, "H-infinity controller based disturbance rejection in continuous stirred-tank reactor," *Intelligent Automation & Soft Computing*, vol. 31, no.1, pp. 29–41, 2022.
- [20] S. Hans, S. Ghosh, S. Bhullar, A. Kataria, V. Karar et al., "Hybrid energy storage to control and optimize electric propulsion systems," *Computers, Materials & Continua*, vol. 71, no.3, pp. 6183–6200, 2022
- [21] S. Hans, S. Ghosh, A. Kataria, V. Karar and S. Sharma, "Controller placement in software defined internet of things using optimization algorithm," *Computers, Materials & Continua*, vol. 70, no.3, pp. 5073– 5089, 2022
- [22] Sikander Hans, Balwinder Singh, Vivek Parihar, Sukhpreet singh "Human-AI Collaboration: Understanding User Trust in ChatGPT Conversations" *IJSREM*, vol. 8 no 1,2024,pp-1-14.
- [23] Sikander Hans. Balwinder singh "Enhanced Load Frequency Control in Isolated Micro-Grids Using ANFIS Controller for Stability and Efficiency", *International Journal of Applied Science and Technology Research Excellence IJSREM*, vol. 12 no 6 ,2023, pp-1-18
- [24] Saurbh, Ankush, Pankaj, Sikander Hans " Engineering Solutions for Mountainous Road Construction: A Comprehensive Study on Geophysical and Geotechnical Factors Influencing Slope Stability" *IJSREM*, Vol. 7, no. 12, pp- 1-14.
- [25] Balwinder Singh, Sikander Hans "Comparative Study of THD Characteristics in Different Cascaded H-Bridge Configurations for Multilevel Multicarrier Modulation" *IJSREM*, vol. 8 no 2,2024, pp-1-21.
- [26] Ooi, C. A., Rogers, D., & Jenkins, N. (2015). Balancing control for grid-scale battery energy storage system. *Proceedings of the Institution of Civil Engineers-Energy*, 168(2), 145-157.
- [27] Habib, A. A., Hasan, M. K., Mahmud, M., Motakabber, S. M. A., Ibrahimya, M. I., & Islam, S. (2021). A review: Energy storage system and balancing circuits for electric vehicle application. *IET Power Electronics*, 14(1), 1-13.
- [28] Chen, F., Deng, H., & Shao, Z. (2020). Decentralised control method of battery energy storage systems for SoC balancing and reactive power sharing. *IET Generation, Transmission & Distribution*, 14(18), 3702-3709.
- [29] Chen, F., Deng, H., & Shao, Z. (2020). Decentralised control method of battery energy storage systems for SoC balancing and reactive power sharing. *IET Generation, Transmission & Distribution*, 14(18), 3702-3709.
- [30] Morstyn, T., Momayyezani, M., Hredzak, B., & Agelidis, V. G. (2015). Distributed control for state-of-charge balancing between the modules of a reconfigurable battery energy storage system. *IEEE Transactions on Power Electronics*, 31(11), 7986-7995.